SRNL-STI-2010-00050

Relative Humidity and the Susceptibility of Austenitic Stainless Steel to Stress Corrosion Cracking in an Impure Plutonium Oxide Environment

P. E. Zapp,[1] J. M. Duffey,[1] P. S. Lam,[1] K. A. Dunn,[1]
D. K. Veirs,[2] L. A. Worl,[2] and J. M. Berg[2]

Savannah River National Laboratory[1]
Aiken, SC 29808
and
Los Alamos National Laboratory[2]
Los Alamos, NM 87545

Philip E. Zapp
Fellow Engineer
Savannah River National Laboratory
Ph. D. in Metallurgical Engineering, University of Illinois at Urbana-Champaign
B. A. in Physics, Cornell University

Jonathan M. Duffey
Principal Scientist
Savannah River National Laboratory
Ph.D. Inorganic Chemistry, University of Tennessee
M.S. Inorganic Chemistry, University of Tennessee
B.S. Chemistry, Union University

Poh Sang Lam
Senior Fellow Engineer
Savannah River National Laboratory
Ph.D. Theoretical and Applied Mechanics, University of Illinois at Urbana-Champaign
M.S. Engineering and Applied Science, Yale University
B.S. Naval Architecture & Marine Engineering, National Cheng Kung University Taiwan

Kerry A. Dunn
Advisory Engineer
Savannah River National Laboratory
M.S. Materials Science and Engineering
B.S. Metallurgy, Pennsylvania State University.

D. Kirk Veirs
Staff Scientist
Los Alamos National Laboratory.
Ph.D. Physical Chemistry, Pennsylvania State University
B.S. Chemistry and Environmental Science, Northern Arizona University

Laura A. Worl
Project Manager.
Los Alamos National Laboratory
Ph.D. Chemistry, University of North Carolina
B.S. Chemistry, Magna Cum Laude, University of Delaware
John M. Berg
Staff Scientist
Los Alamos National Laboratory, Los Alamos, NM
PhD Chemistry, Princeton University
B.A. Chemistry, St. John's University

ABSTRACT

Laboratory tests to investigate the corrosivity of moist plutonium oxide/chloride salt mixtures on 304L and 316L stainless steel coupons showed that corrosion occurred in selected samples. The tests exposed flat coupons for pitting evaluation and "teardrop" stressed coupons for stress corrosion cracking (SCC) evaluation at room temperature to various mixtures of PuO_2 and chloride-bearing salts for periods up to 500 days. The exposures were conducted in sealed containers in which the oxide-salt mixtures were loaded with about 0.6 wt % water from a humidified helium atmosphere. Observations of corrosion ranged from superficial staining to pitting and SCC. The extent of corrosion depended on the total salt concentration, the composition of the salt and the moisture present in the test environment. The most significant corrosion was found in coupons that were exposed to 98 wt % PuO_2, 2 wt % chloride salt mixtures that contained calcium chloride and 0.6 wt% water. SCC was observed in two 304L stainless steel teardrop coupons exposed in solid contact to a mixture of 98 wt % PuO_2, 0.9 wt % NaCl, 0.9 wt % KCl, and 0.2 wt % $CaCl_2$. The cracking was associated with the heat-affected zone of an autogenous weld that ran across the center of the coupon. Cracking was not observed in coupons exposed to the headspace gas above the solid mixture, or in coupons exposed to other mixtures with either no $CaCl_2$ or 0.92 wt% $CaCl_2$. SCC was present where the 0.6 wt % water content exceeded the value needed to fully hydrate the available $CaCl_2$, but was absent where the water content was insufficient.

These results reveal the significance of the relative humidity in the austenitic stainless steels' environment to their susceptibility to corrosion. The relative humidity in the test environment was controlled by the water loading and the concentration of the hydrating salts such as $CaCl_2$. For each salt or salt mixture there is a threshold relative humidity below which the necessary liquid electrolyte cannot exist, and therefore below which the SCC risk is very low. This threshold is a thermodynamic quantity known as the deliquescence relative humidity that is dependent on the identity of the salt but is independent of the quantity of salt. Below the deliquescence RH there should be low corrosion risk, and above it the corrosion risk increases rapidly as a liquid phase, which is initially saturated with salt, grows and becomes more widespread in the container.

INTRODUCTION

The stress corrosion cracking (SCC) of austenitic stainless steels has been extensively studied, especially in acidic aqueous chloride solutions, and is described in a large body of literature.[1] Although SCC is most frequently investigated in a wide variety of bulk liquid phase environments, there has been interest in exploring the phenomenon where the corrosive electrolyte derives from humid atmospheres. Stress corrosion cracking in such instances is of particular interest in the safe containment and storage of impure plutonium oxides in austenitic stainless steel vessels, where the impurities include hydrophilic chloride salts.

As discussed in the previous issue of this journal,[2] the United States Department of Energy Standard DOE-STD-3013-2004 "Stabilization, Packaging and Storage of Plutonium-Bearing Materials" (the '3013' standard) specifies the processing steps and storage vessel attributes that are required for the storage of plutonium metal and oxides. These include the heat treatment of the oxide mixtures to reduce water content and the use of at least two nested, welded containers fabricated from corrosion resistant alloy(s). In practice the inner of the two containers has been fabricated from either 304L or 316L stainless steel, and the outer has been fabricated of 316L stainless steel. The Pu-oxide heat-treatment requires heating to 950°C for at least two hours in an oxidizing atmosphere. The heat-treated material shall contain less than 0.5% by weight water, and that limit must be maintained through the packaging and sealing of the material within the two containers. Both inner and outer containers are sealed by welding, and the 3013 standard specifies leak-tightness limits.

A portion of the plutonium oxide inventory may contain chloride salts in significant concentration, so that there is the potential of an aqueous electrolyte containing chloride ions in contact with the stainless steel containers, if there is sufficient moisture in the sealed 3013 container to exceed the deliquescence relative humidity of the salts in the container. For austenitic stainless steels, such an electrolyte can induce localized modes of corrosion such as pitting and stress corrosion cracking, as well as crevice corrosion. Ninety days of exposure to PuO_2/Cl^- salt mixtures can produce pitting in small-scale 304L stainless steel vessels.[3] Pitting depths up to 100 μm were observed on the metal surface in contact with the solid oxide and up to 25 μm on metal exposed to the vapor space above the solid. Testing of flat coupons showed that 304L stainless steel exposed at 55°C to salt mixtures with approximately 0.5 wt % moisture suffers pitting corrosion to a maximum depth of 30 μm in an area in contact with the solid mixture.[4] The flat coupons were exposed for 150 days. Additionally, a 316L coupon exposed to similar conditions had a small area (2 by 4 mm) of pitting of about 10 μm in depth. Coupons of both 304L and 316L stainless steel exposed at room temperature were either not corroded or had barely detectable attack. Specimens under tensile stress were not investigated in those early tests.

This paper describes the results of coupon immersion tests that investigated stress corrosion cracking as well as pitting in moist plutonium oxide/chloride salt mixtures. The objective was to determine the effects of chloride salt composition and radiation on

the corrosion of 304L and 316L austenitic stainless steel and to refine the understanding of the relative importance of the concentrations of NaCl, KCl, $MgCl_2$, and $CaCl_2$, water content, and radiation dose to the corrosion-cracking process.

The small-scale test program included the following five test series (Table 1):

Series 1 included one test container (series 1a) with a PuO_2 sample with no chloride salts as an experimental control. The two other containers in this series (series 1b) contain a composition of PuO_2 with 28 wt % chloride salts composed largely of non-hydrating NaCl and KCl with some $CaCl_2$ and $MgCl_2$.

Series 2a tests contained PuO_2 with 5 wt % NaCl and 5 wt % KCl.

Series 3 tests evaluated the impact of the hydrating salt $MgCl_2$ on the corrosion of stainless steel using a laboratory-prepared surrogate of PuO_2 and salts intended to be representative of salts produced by the electrorefining process (termed 'ER' salt). Three compositions of the PuO_2/ER salt mixture that contained equal weight NaCl/KCl and $MgCl_2$ equal to one tenth of the total salt content were tested:

Series 3a) 90 wt % PuO_2 + 10 wt % ER salt
Series 3b) 95 wt % PuO_2 + 5 wt % ER salt
Series 3c) 98 wt % PuO_2 + 2 wt % ER salt

Series 4 tests assessed to assess the role of $CaCl_2$, another hydrating salt, versus that of $MgCl_2$ in the overall salt composition. The total salt concentration was 2 wt % in the series 4 tests, with two variants containing different concentrations of $CaCl_2$. Series 4a contained 0.2 wt % $CaCl_2$, and series 4b 0.92 wt % $CaCl_2$.

Series 5a tests evaluated the impact of increased α-dose on corrosion during exposure to the series 3b oxide/salt composition. Series 5a used a 5 wt % $MgCl_2$-rich ER salt with the mixture's specific radioactivity increased by the addition of Pu-238 and Am-241 to the standard Pu-239 isotope used in the preparation of the oxide. The addition of Pu-238 and Am-241 increased the thermal power of this isotopic mixture from 2.26 W/kg Pu for the weapons grade mixture used in the series 1 through 4 tests to 5.09 W/kg Pu in the series 5a tests.

TABLE 1
TEST SERIES SOLID MIXTURE COMPOSITIONS (WEIGHT %)

Series	Description	PuO_2	NaCl	KCl	$MgCl_2$	$CaCl_2$
1a	Control, 0% salt	100	–	–	–	–
1b	master blend	72	11.7	14.8	1.1	0.4
2a	10% NaCl/KCl	90	5.0	5.0	–	–
3a	10% ER Salt	90	4.5	4.5	1.0	–
3b	5% ER Salt	95	2.25	2.25	0.50	–
3c	2% ER Salt	98	0.90	0.90	0.20	–
4a	2% Ca Salt	98	0.90	0.90	–	0.20
4b	2% 11589 Salt	98	0.54	0.54	–	0.92
5a	5% ER Salt	95	2.25	2.25	0.5	–

ROLE OF RELATIVE HUMIDITY

The risk of SCC in stressed stainless steel is very low in the absence of direct contact of the metal with a liquid phase that can serve as an electrolyte for the corrosion process. Therefore, a major goal of this test plan is to better define whether a liquid phase could be present in any 3013 containers given current knowledge about packaging conditions, container contents, and storage conditions.

Internal relative humidity (RH) is a useful indicator of the potential existence of an aqueous liquid phase anywhere in a container. For each salt or salt mixture there is a threshold relative humidity below which a liquid cannot exist and, therefore, below which the SCC risk is very low. This threshold is a thermodynamic quantity known as the deliquescence relative humidity and is dependent on the identity of the salt but is independent of the quantity of salt. Below the deliquescence RH there should be low corrosion risk, while above the deliquescence RH the corrosion risk increases rapidly as the liquid phase forms and becomes more widespread in the container. At extremely high relative humidity the risk may fall due to the formation of less corrosive dilute salt solutions. However, the relative humidity at which the risk falls is dependent on the quantity of salt in the container. (Note that the concept of a maximum safe chloride concentration is problematic due to possible concentrating mechanisms such as thermal cycling.)

Figure 1 shows a conceptual plot of how SCC risk might vary with the container internal relative humidity for two general categories of impurity phases. The first category (dotted line in Figure 1) contains only alkali chloride salts (NaCl, KCl) and is expected to represent little risk within the range of packaging relative humidities because an aqueous salt solution will not form. The second category (solid lines in Figure 1) includes alkaline earth chloride (AEC) materials with pure alkaline earth chlorides ($MgCl_2$, $CaCl_2$)

and mixed salts containing alkaline earths ($KMgCl_3$, $KCaCl_3$, etc.), which are known to form aqueous chloride solutions within the range of packaging relative humidities. These materials represent the greatest risk for SCC within the range of packaging relative humidities. Figure 1 and subsequent plots are based on published thermodynamic studies of chloride salts and water, and on corrosion studies conducted in Japan which observed stainless steel SCC in contact with alkaline earth chloride salts at room temperature.[5]

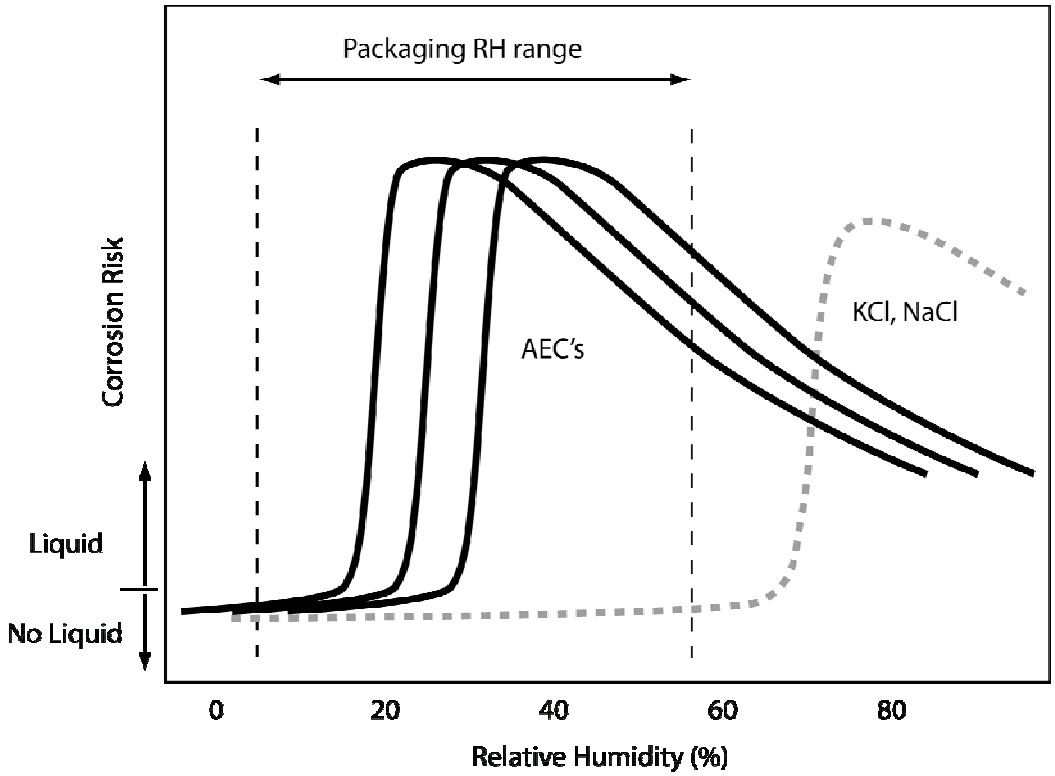

Figure 1: Conceptual plot of corrosion risk as a function of relative humidity within a container. Curves are shown for alkali chlorides (NaCl, KCl) [Dotted line] and for a representative collection of alkaline earth chlorides (labeled AEC's) [Solid lines]. Risk is shown as increasing rapidly beginning at the threshold for liquid formation (deliquescence). The range of relative humidity to which material was exposed during packaging is shown for comparison.

The range of relative humidity experienced during packaging spans the known deliquescence relative humidity values of all the calcium and magnesium chloride salts likely to be present in packaged material. Therefore SCC must be considered as possible within existing containers based on this simple thermodynamic picture. Several mitigating factors may effect actual 3013 packages, including the potential decline in the internal relative humidity, due to radiolysis of water after container closure, to values substantially below the packaging relative humidity and perhaps below the deliquescence relative humidity of any impurity salts. Establishing reliable methods to estimate this reduction in relative humidity, as well as better defining the range of plausible

deliquescence thresholds of real stored material is the most promising approach to reducing the overall concern and, through knowledge of the package contents, limiting the concern to the fewest possible number of specific containers.

Relative humidity within a container is controlled by an affinity and capacity for water that is characteristic of each of the solid constituents in the package. Figure 2 shows simplified examples where $CaCl_2$ is the only solid constituent that interacts with water. As moisture is added to the system the dry salt is converted into solid hydrates, with stepwise increases in RH evident as each formation step is completed. Once the salt is fully hydrated, further moisture addition begins to form a saturated salt solution at a constant RH characteristic of the deliquescence RH of the salt. Eventually the salt will be fully dissolved and further moisture addition will be characterized by a smooth increase in RH as the solution becomes more dilute.

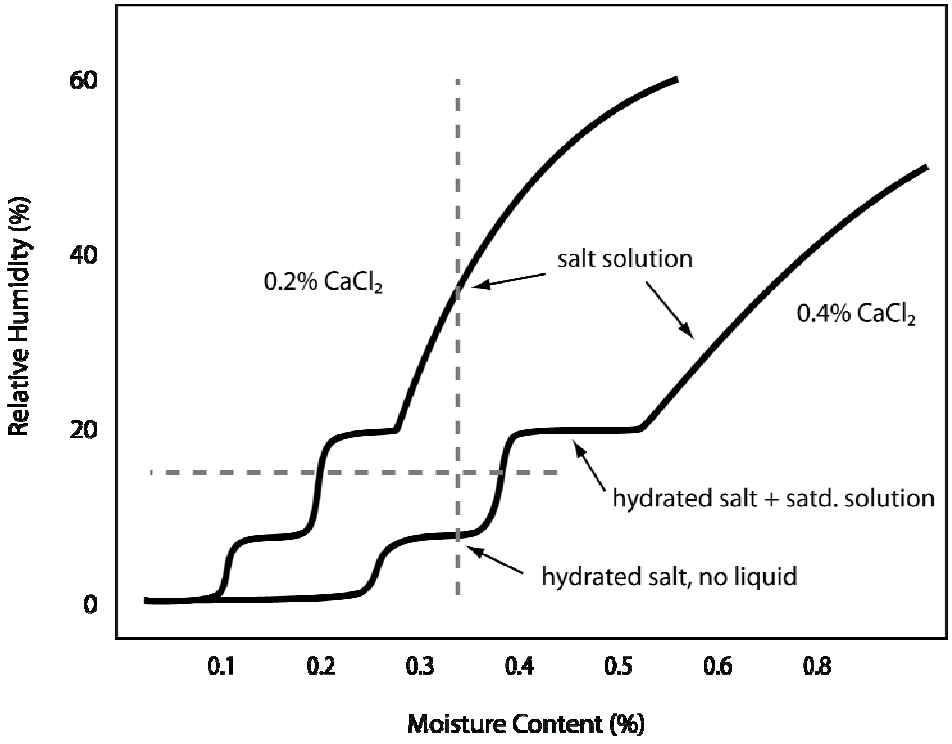

Figure 2: Relative humidity vs. moisture content for two mixtures of $CaCl_2$ with an inert matrix.

Comparison of the two curves in Fig. 2 illustrates the difficulty of attempting to use total moisture content to estimate SCC risk. At a moisture content of 0.34%, indicated by the vertical dashed line in Fig. 2, the 0.2% $CaCl_2$ material would contain an aqueous salt solution phase while all the H_2O will be tied up in solid hydrates of the 0.4% $CaCl_2$ material, so the corrosion risk would be very different in these two cases. An analogous plot for a real packaged batch of material would be more complex due to multiple impurity phases but the conclusion would be the same. To relate the existence or absence

of a liquid phase to overall moisture content, one must also know the quantities of those impurity phases that interact most strongly with H_2O, not just their identities. Since there is little prospect of adequately quantifying important impurity phases in individual containers from existing data, moisture content alone is not a promising predictor of the potential for liquid formation, and therefore the SCC risk will also be difficult to predict.

Bounding estimates of internal RH, in contrast, would be good predictors of the potential for existence of an aqueous liquid phase even without knowledge of the quantities of the impurity phases. For example, at or below the RH indicated by the horizontal dashed line in Fig. 2 no solution could exist regardless of how much or how little $CaCl_2$ is present in these hypothetical material mixtures. The added complexity of actual packaged material will not alter the basic premise as long as the identities of the phases can be reasonably constrained by existing information. As long as the upper bound for potential internal RH does not exceed the deliquescence relative humidity of any plausible impurity phases, an aqueous liquid phase will not exist in the container. This approach avoids what would be a highly problematic effort to quantify minor impurity phases in individual containers.

Figure 3 shows a conceptual model of SCC risk versus moisture content for the same two hypothetical material compositions shown in Fig. 2. The main change in risk occurs due to liquid formation and is seen to occur at dramatically different moisture loadings for the two mixtures. An analogous plot versus internal relative humidity, as in Fig. 1, would show the rise in risk occurring at the same RH for both mixtures.

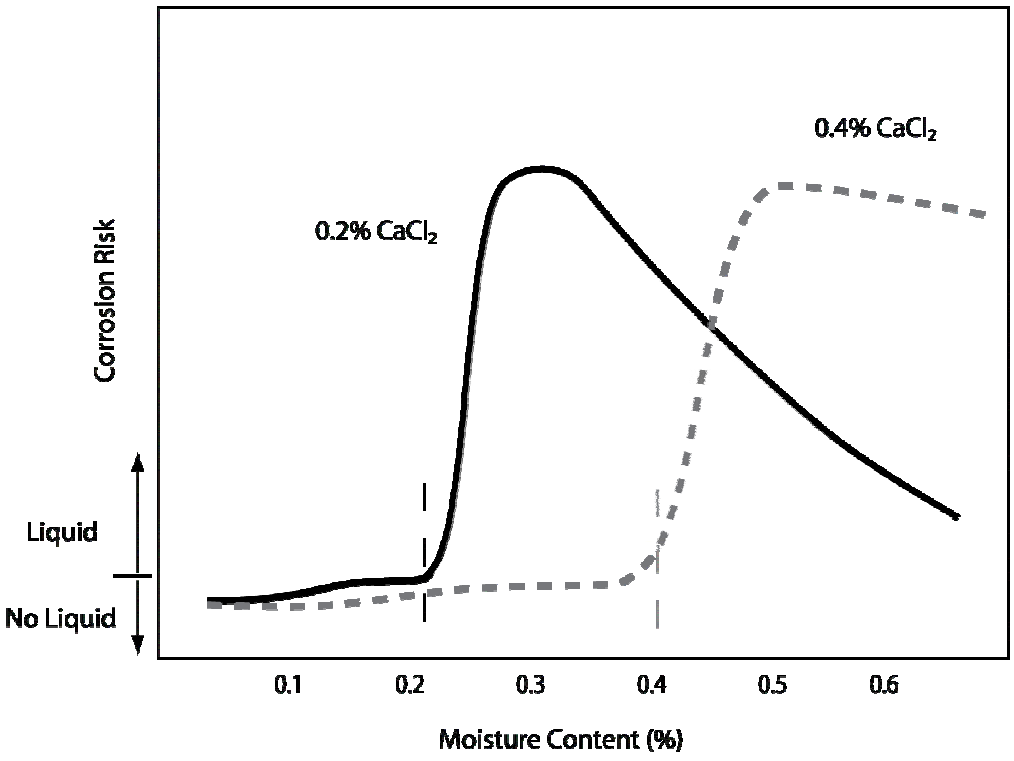

Figure 3: Conceptual plot of relative corrosion risk as a function of total moisture content for two batches with different loading of $CaCl_2$ and no other active salt.

Note that corrosion risk is strongly dependent on the amount of active salt and can be significant well below 0.5 wt % moisture. The dashed vertical lines indicate the approximate moisture loadings above which solution exists in the two cases.

EXPERIMENTAL PROCEDURE

The corrosion tests used 304L and 316L stainless steel coupons purchased from Metal Samples Inc., Munford AL. Pitting corrosion was evaluated with 1-inch by 2-inch by 0.06-inch flat coupons with a longitudinally centered autogenous weld (ground flat to the coupon surface with a 600-grit finish). The weld penetration was approximately 0.03 inches or half way through the plate sample. SCC was evaluated with a "teardrop" specimen, a type of compact U-bend specimen with its ends welded together to hold the stressed bend. The metal was plastically deformed during bending around a mandrel. An analysis of the stresses within the specimen is discussed below. The teardrop specimens had a transverse autogenous weld at the center of curvature.

The test container for the small-scale tests was a 5-cm (2-inch) diameter, 6.5-cm (2.5-inch) tall stainless steel can sealed with a metal gasket. The container was equipped with a pressure transducer for continuous pressure monitoring during an exposure and a valve for acquiring gas samples periodically (Figure 4). Glass inserts were used to hold the small (several cubic-centimeter) volumes of oxide/salt mixture (allowed under limits on the fissile material mass) to maximize the surface area of contact with the test coupons.

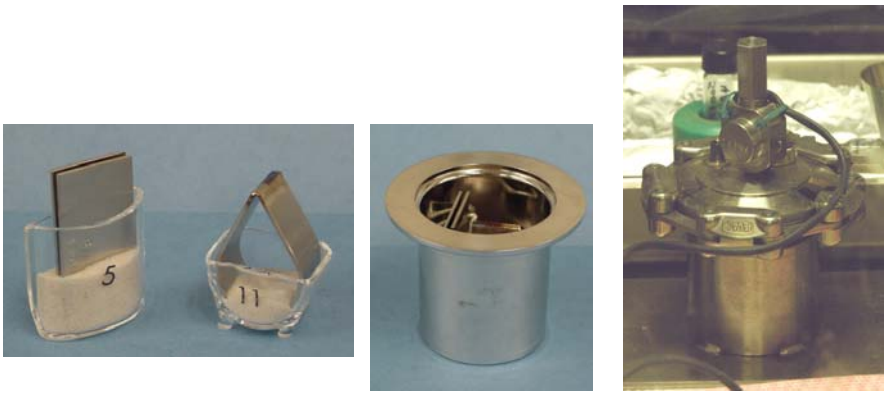

Figure 4. Flat and teardrop coupons in glass inserts, open test container, and sealed container.

Figure 4 shows the coupons in their glass boats or inserts and an open test container with coupons. One 304L flat coupon and one 316L flat coupon were placed side by side in one glass insert. Enough oxide/salt mixture was added between and around the coupons to cover the lower half of each coupon. Several grams of oxide/salt mixture were added to a second glass insert, and one teardrop coupon was placed in this second glass insert on top of the oxide/salt mixture. Several more grams of oxide/salt mixture were added inside the closed loop of the teardrop coupon. The two glass inserts were placed side by side in the vessel. A second teardrop coupon was then placed on top of the first such that it rested in the headspace position without contacting the oxide/salt mixtures.

PuO_2 was prepared by anion exchange purification, oxalate precipitation, and calcination in a dry air purge for two hours at 950°C. Various salt mixtures having the desired ratios of NaCl, KCl, $MgCl_2$, and $CaCl_2$ were prepared by combining the required amounts of each salt in a glovebox with a dry argon atmosphere. The dry salt mixtures were then removed from the glovebox in a desiccator and heated in a static air atmosphere to between 820°C and 850°C for two hours to melt the salts together. While still warm, the fused salts were placed back in the desiccator and transferred back to the dry glovebox where they were ground and pre-weighed into screw-cap glass vials. The pre-weighed salt mixtures were transferred to a plutonium glovebox where they were combined with pre-weighed amounts of PuO_2 in screw-cap jars, mixed briefly while the jars were capped, then transferred to a crucible and placed directly in a warm furnace. The PuO_2/salt mixtures were heated in a static air atmosphere at 850°C for two hours, cooled to approximately 300°C, and transferred to screw-cap glass jars.

A helium-purged glove bag deployed inside a plutonium glovebox was used to provide a helium atmosphere for loading PuO_2/salt mixtures and corrosion test coupons into the test containers. The glove bag was first purged with helium until the relative humidity (RH) was below 10%. PuO_2/salt mixtures were then weighed into glass inserts containing the corrosion test coupons as previously described. The two glass inserts in each sample set were placed in small stainless steel pans for ease of handling. The RH in the glove bag was gradually increased by bubbling helium through a container of distilled water and/or by moistening absorbent wipes with water and spreading them out in a large stainless steel pan to speed evaporation of water. The small stainless steel pans holding the sample sets were weighed periodically in the humidified helium atmosphere until the weight gain of each sample set corresponded to uptake of about 0.6 wt% water. This moisture content was selected because it was slightly above the allowable moisture in the 3013 containers. A “blank” consisting of pan, glass inserts, and test coupons with no PuO_2/salt mixture was weighed along with each set of exposed samples to estimate the amount of water adsorbed by the container and coupons surfaces. The maximum RH required for samples to reach the target moisture loading in a nominal eight-hour shift was between 58% and 94%. The containers, with their moisture loadings, were closed and transferred to air atmosphere gloveboxes for ambient temperature staging.

RESULTS

Corrosion observations and an analysis of the water content of the test containers that have completed their exposures were made after the containers were opened. These containers had been at ambient glovebox temperature for between 150 and 506 days. Prior to opening each container, the headspace gas in the container was diluted with helium and sampled for analysis. The post-exposure water content of samples of the PuO_2/salt mixtures was measured by thermogravimetric analysis coupled with mass spectrometric detection (TGA-MS), typically within one to three days after opening the container. During this interval the samples were in screw-lid sealed glass vials.

Upon completion of their exposures, the stainless steel coupons were examined visually and photographed. The coupons were lightly brushed to remove oxide/salt mixture, and cleaned of corrosion product with 0.1 M nitric acid. Observations of corrosion are summarized in Table 2 below. Corrosion ranged from slight, superficial staining in the series 1 tests to pitting with measurable depth and SCC in the 304L coupons in the series 4a containers. There was no significant qualitative difference in the pitting attack on the 304L and 316L stainless steels, and the depth of attack measured on all the flat coupons was comparable. The only extensive pitting was in coupons exposed to PuO_2/Cl^- salt mixtures with 2 wt % total salt that included $CaCl_2$ (the 4a and 4b series tests). Although not quantified, pitting was observed on the teardrop coupons in containers whose flat coupons were pitted.

TABLE 2
SUMMARY OF CORROSION OBSERVATIONS

Test Container	Salt Content	Days Sealed	Corrosion Observations of Tear Drop Coupons
1a-1	None	325	no cracking (304L)
1b-1	28% salt	489	no cracking (304L)
1b-2		150	no cracking (304L)
3c-1	2% ER Salt	274	no cracking (304L)
4a-1	2% Salt with 0.2% $CaCl_2$	506	no cracking (316L), pitting
4a-2		335	cracking (304L) in solid contact region, pitting
4a-3		166	cracking (304L) in solid contact region, pitting
4b-1	2% Salt with 0.9% $CaCl_2$	193	no cracking (304L), pitting
4b-2		340	no cracking (304L), pitting
4b-3		496	no cracking (304L), pitting
5a-1	5% ER Salt with increased α-dose	352	no cracking (304L), pitting
5a-2		168	no cracking (304L), pitting
5a-3		470	no cracking (304L), pitting

Stress Corrosion Cracking Observations

Teardrop coupons were used to assess the susceptibility of 304L stainless steel to SCC induced by the moist oxide/salt mixture. Two teardrop coupons, one from container 4a-3 and one from container 4a-2, were found to have undergone SCC after 166 and 335 days of exposure, respectively, in the solid contact position. Cracking was not observed in coupons from any other container opened to date, nor was cracking seen in any headspace-position coupon, even in the coupons exposed in containers 4a-3 and 4a-2. Cracking was not observed in the 316L teardrop coupons exposed to mixture 4a-1.

In general, all teardrop coupons had staining and pitting similar in extent to that seen in their companion flat coupons. Some teardrop coupons had general staining or corrosion in the heat-affected zones of their closure weld. Figures 5 and 6 show examples of the pitting and staining in teardrop coupons exposed in the solid contact positions in containers 4a-3 and 4b-1. These images were made before acid cleaning of the coupons. Pitting is visible on the outer and inner curved surfaces of the coupons as well as at edges.

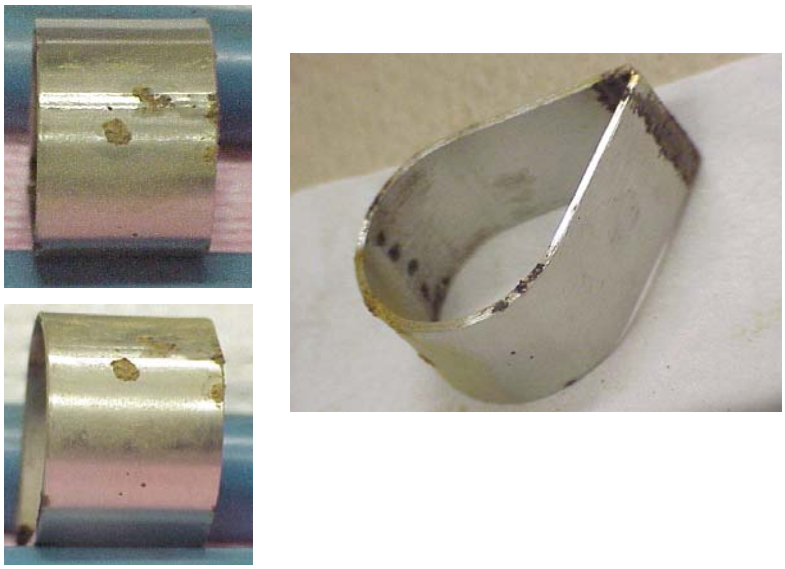

Figure 5. Container 4a-3 teardrop coupon 304L – 23 showing pitting in the metal in contact with the oxide/salt mixture. Corrosion is also evident in the heat-affected zone of the closure weld at the coupon tip, which was not in contact with the solid mixture.

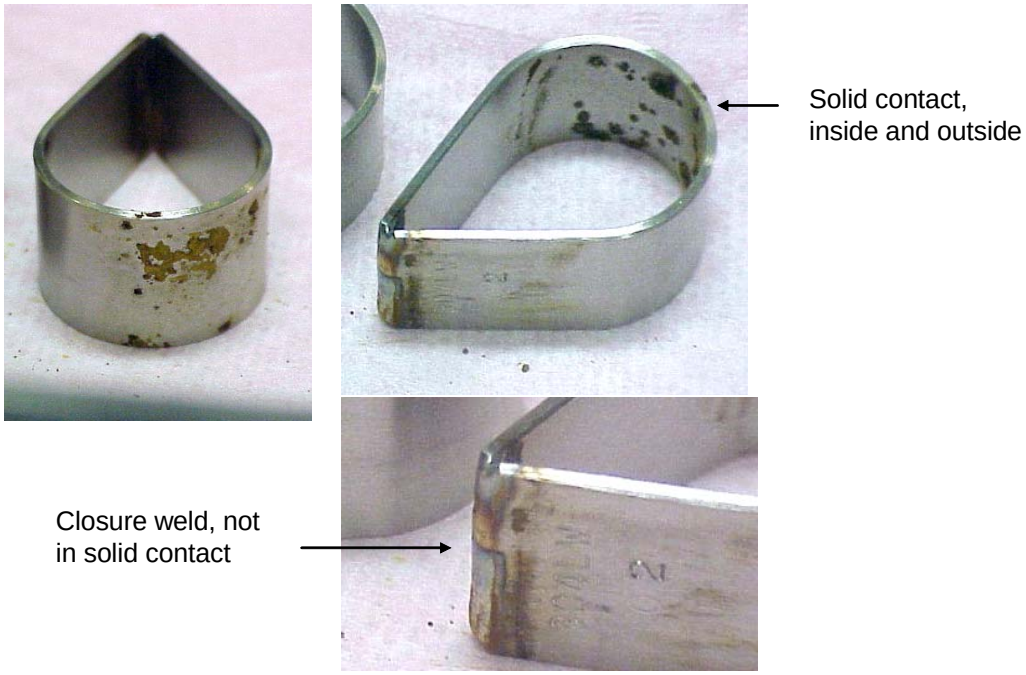

Figure 6. Container 4b-1 teardrop coupon 304L – 02 showing pitting inside and outside in metal in solid contact; no evidence of cracking; staining near closure weld.

Stress corrosion cracking was initially revealed in the container 4a-3 solid contact teardrop coupon 304L – 23, through dye penetrant testing.[6] Optical microscopy, scanning electron microscopy, and optical metallography were used to examine the path and nature of the cracking.[7] The cracking extended across more than half the width of the coupon and was associated with the transverse autogenous weld. Figure 7 is an optical micrograph that shows the cracking starting at the edge of the coupon in a localized area of general corrosion and propagating along the interface between the weld and the parent metal, that is, in the weld heat-affected zone. Figure 8 shows the entire crack path on the coupon surface in a composite scanning electron micrograph. The crack was highly branched as it crossed through weld metal and continued its path along the opposite weld/parent metal interface. Optical metallography of one cross-section of the coupon reveals the propagation of the crack along the interface (Figure 9) and, in a second cross-section, propagation through the weld metal into the parent metal (Figures 10 and 11). The enlargement in Figure 10 shows what appears to be intergranular cracking around grains in the weld heat-affected zone. This possible intergranular cracking can result from the sensitization of the 304L stainless steel by the welding heat input. Sensitization is the phenomenon of the depletion of the protective chromium content of the alloy matrix by concentrating the chromium in chromium carbides that precipitate at grain boundaries. The highest magnification image (Figure 12) shows the extensive cracking paths across parent metal grains. The generally transgranular nature of the cracking is characteristic of chloride-induced SCC in non-sensitized austenitic stainless steel.

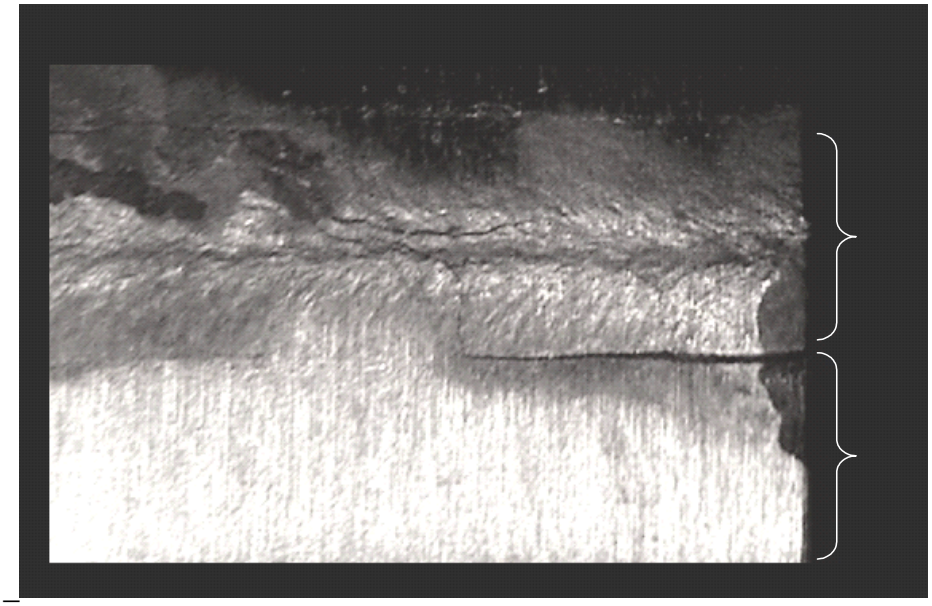

Figure 7. Photomicrograph of teardrop coupon 304L – 23, showing branched cracking near and within the autogenous weld; possible crack initiation site in area of localized corrosion at right edge of coupon. Approximately 10X magnification.

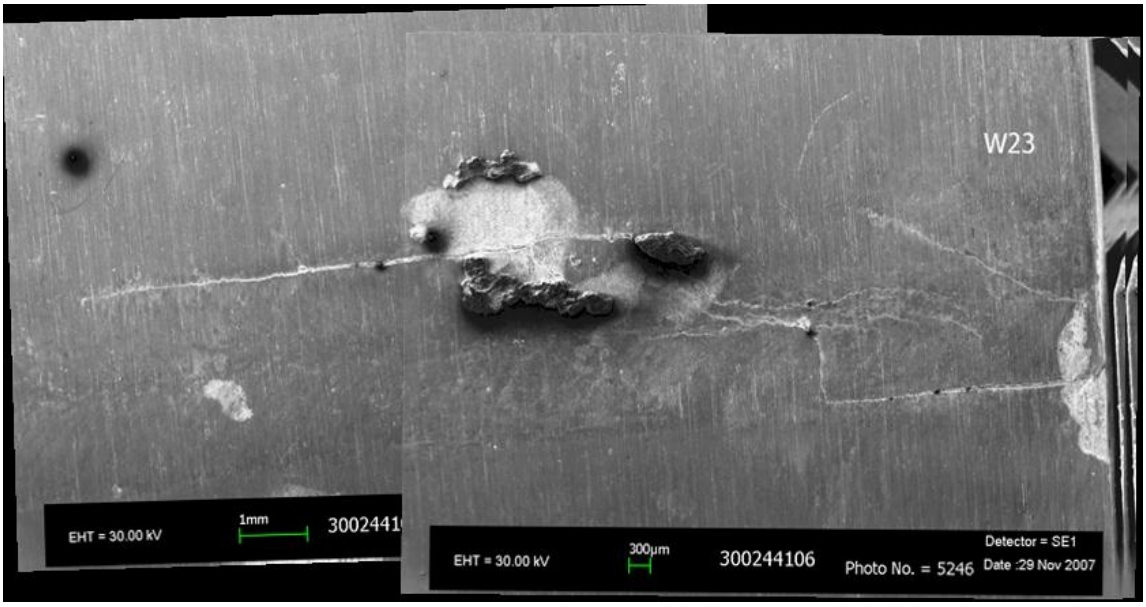

Figure 8. Composite scanning electron micrographs of coupon 304L-23 showing full extent of cracking on outside (convex) surface.

Figure 9. Scanning electron micrograph of edge of coupon 304L-23 showing cracking along weld/parent metal interface.

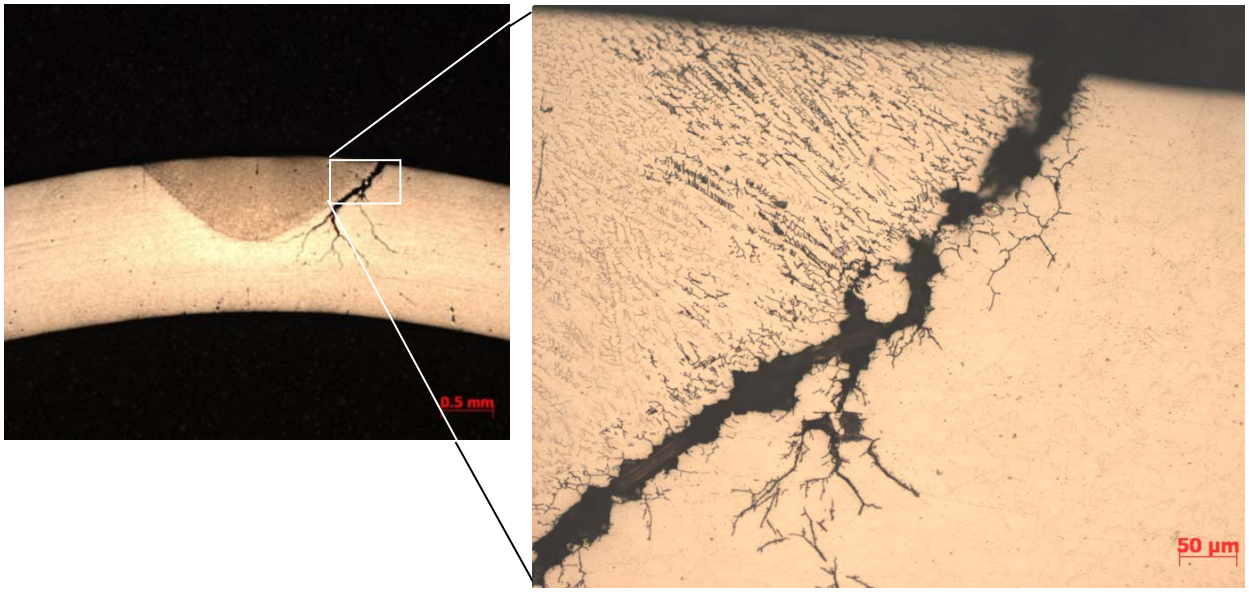

Figure 10. Optical micrographs of a reversed cross-section through teardrop coupon 304L-23 showing cracking along the weld/parent metal interface.

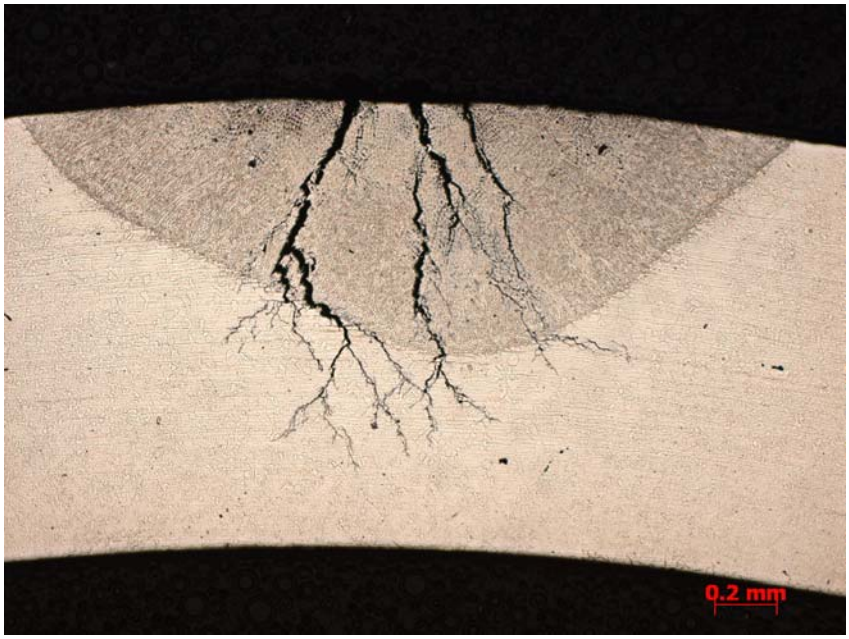

Figure 11. Optical micrograph of a second cross-section of coupon 304L – 23, showing propagation of multiple cracks through the weld metal into the parent metal.

Figure 12. Optical micrograph showing transgranular nature of the cracking.

Similar SCC occurred in a second series 4a test coupon, 304L – 20 from container 4a-2, which was exposed for 335 days or about twice the exposure of container 4a-3. Figure 13 shows the prominent stress corrosion cracks at the weld metal/parent metal interfaces of the coupon. A third series 4a container, container 4a-1, held 316L stainless teardrop coupons in both the solid contact and headspace positions for 506 days. Although teardrop coupon 316L – 40 experienced extensive pitting and localized general corrosion, visual inspection revealed no cracking. Type 316L stainless steel contains molybdenum to impart resistance to chloride attack. This resistance takes the form of a greater induction time for SCC rather than immunity to SCC.

.

Figure 13. Stress corrosion cracking along the autogenous weld in coupon 304L – 20 from container 4a-2.

As stated above, SCC has not been observed in 304L teardrop coupons that were exposed in any containers other than 4a-2 and 4a-3. Notably, cracking was absent from coupons exposed in the 4b test containers, whose PuO_2/Cl^- salt mixtures contained $CaCl_2$ at a concentration of 0.92 wt% compared with 0.2 wt% $CaCl_2$ in the 4a containers. Clearly a corrosive electrolyte did form in container 4b-1, and considerable corrosion is evident in the stressed region of its teardrop coupon. The reason for the absence of cracking in this instance is not known, but further testing at elevated temperature (of the order of 70°C) must be conducted to draw conclusions about the corrosivity of the 0.92 wt% $CaCl_2$ mixture. The results at room temperature show that oxide/salt mixtures containing $MgCl_2$ rather than $CaCl_2$ (the series 3 tests and the series 5 tests, with their higher radiation level) did not initiate SCC.

Stress Analysis of Teardrop Coupon

A finite-element analysis was used to estimate the initial stress in the 304L tear drop specimens in which cracking occurred.[8] The ABAQUS program was used to perform the finite element analysis.[9] Only one-half of the 304L strip and one-half of the mandrel are needed in the finite element calculation because of geometric symmetry. The stress analysis was based on the fabrication of the teardrop coupon by the bending of a starting 10-cm-long strip around a 2.5-cm-diameter mandrel. The 0.2% offset yield stress for the 304L stainless steel is 351 MPa (50.93 ksi), the ultimate tensile strength (UTS) is 662 MPa (96.05 ksi), and the elongation (at fracture) with a 50.8 mm (2 in.) gage length is 45.85%. The full stress-strain curve necessary for the finite element analysis was not provided. A preliminary assessment of the stress state of the tear drop specimen was made without material-specific testing. A stress-strain curve with similar values of yield stress (455 MPa or 66 ksi) and ultimate tensile strength (689 MPa or 100 ksi) was used for the present analysis. The tensile properties of the small volume of autogenous weld metal were assumed to be the same as those of the base metal (304L).

It was determined that the maximum stress level is about 731 MPa (106 ksi). The highest bending stress in the tear drop specimen is not located at the apex as expected. The finite element analysis showed that the apex stress is relieved and continuously redistributed as the 304L strip is being bent around the mandrel, and the location of the highest stress is shifted from the apex to the specimen shoulders. This is caused by the increasing contact surface between the 304L strip and the mandrel in the course of forming the specimen, which effectively changes the bending moment of the system. The analysis showed that for this specimen geometry, the stress at the apex location of the autogenous weld is about 483 MPa (70 ksi, see the apex stress in Figure 14).

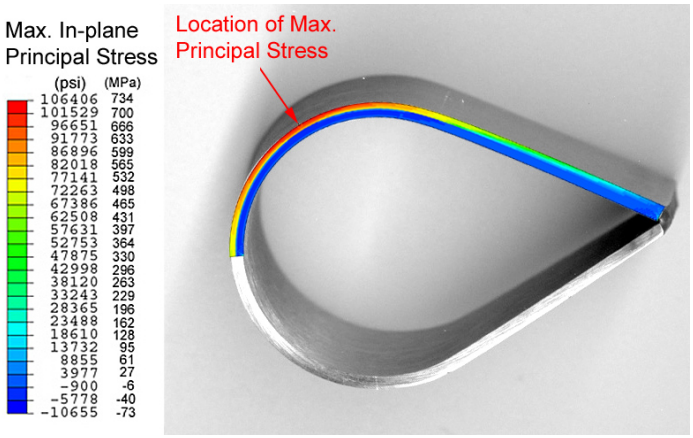

Figure 14. The location of maximum stress in the teardrop specimen. The stress distribution is symmetrical with respect to the plane containing the apex (center of curvature) and the welded ends of the coupon.

That the cracking seen in the 4a teardrop coupons was associated with the autogenous welds and not with predicted highest-stress region may well be associated with microstructural and compositional effects brought about by the weld process, such as the phenomenon of sensitization mentioned above. As reported in the previous issue of this journal, there is sufficient tensile stress throughout the curved region of the teardrop coupon to induce SCC.[10]

Analysis of Water Content

Table 3 shows the analysis of the water content of materials removed from the 13 opened test containers. This net water loading assumes water content prior to exposure to humid atmosphere was negligible. As a cross-check of the initial water content of each sample that was determined by weight gain, the post-exposure water content was measured by TGA-MS analysis and then corrected for water loss via radiolytic or chemical hydrogen production on the basis of headspace gas analysis results. This correction is based on the assumptions that (1) water is the only significant source of hydrogen and (2) one mole of water yields one mole of hydrogen. This correction does not account for water that may have been consumed by chemical reactions to produce, for example, hydroxyl groups on the surface of PuO_2 or oxychloride compounds. The post-exposure moisture content by TGA-MS and the amount of water consumed by hydrogen production were summed to yield a calculated initial water content for each test container, which is the value listed in Table 3. The final column in Table 3 lists the theoretical water content needed to fully hydrate the $MgCl_2$ or $CaCl_2$ present in each container. These values are included for comparison to the measured water contents as an indication of the extent to which (1) the alkaline earth salts were hydrated and (2) a corrosive aqueous electrolyte was formed. The data suggest that the initial water content of the 4a series tests was sufficient to create such an electrolyte, while the higher calcium chloride salt content of the 4b tests bound the available water.

TABLE 3
WATER CONCENTRATION OF PUO_2/SALT MATERIALS (WEIGHT %)

Sample ID	Calculated Initial Water Content	Water Content Fully Hydrated[a]
1a-1	0.38	No salts to hydrate
1b-1	1.00	1.64
1b-2	0.94	1.64
3c-1	0.35	0.23
4a-1	0.58	0.19
4a-2	0.63	0.19
4a-3[i]	0.50	0.19
4b-1	0.66	0.90
4b-2	0.61	0.90
4b-3	0.61	0.90
5a-1	0.49	0.57
5a-2	1.24	0.57
5a-3	0.45	0.57

[a] Fully hydrated is assumed to mean six moles of water for each mole of $MgCl_2$ or $CaCl_2$.

Calculated initial water contents based on post-exposure water analyses were generally equal to or higher than values for initial water added based on weight gain. This is probably because most of the samples contained some amount of moisture prior to exposure to humidified helium. The calculated initial water contents are considered to be more accurate because of the difficulties associated with handling and weighing the samples in the helium glove bag, the high RH required to load up to 0.5 wt % water, and the possibility that some samples had measurable water content prior to moisture uptake.

CONCLUSIONS

Laboratory corrosion tests on room temperature 304L stainless steel coupons exposed to moist (nominally 0.6 wt % water) PuO_2/$CaCl_2$-bearing salt mixtures show that this alloy is susceptible to pitting and SCC under specific conditions of mixture water loading, total chloride salt concentration *and* composition, and physical contact with the solid mixture. Cracking was associated with the heat-affected zone of an autogenous weld in the test coupons. SCC was produced by a mixture containing 98 wt % PuO_2, 0.9 wt % NaCl, 0.9 wt % KCl, and 0.2 wt % $CaCl_2$ (total salt concentration of 2 wt %). Type 316L stainless steel undergoes pitting but not SCC when exposed to this same mixture with similar water loading as in the 304L tests. Type 304L stainless steel showed pitting but did not exhibit cracking under exposure to a mixture with an identical 2 wt % total salt concentration but with a higher $CaCl_2$ concentration of 0.92 wt %. A mixture with a very

high total salt concentration of 28 wt % did not induce pitting or cracking. Cracking was not observed in any coupon that was contacted by headspace gas, but pitting was observed on areas of some coupons that were in headspace gas contact. Pitting measurements on coupons that have been examined microscopically to date showed depths up to 100 μm.

The corrosion tests were conducted in small stainless steel containers that were sealed under a helium atmosphere. At completion of the test, the headspace gas composition was determined, and the water loading of the PuO_2/Cl^- salt mixture was evaluated. Actual water loading of the PuO_2/Cl^- salt mixtures ranged from 0.35 to 1.24 wt %. These values represent gravimetric data corrected with the results of the headspace gas analysis, in particular analysis of hydrogen gas generation from water radiolysis.

The corrosion results and water analyses point to the significance of the relative humidity of the test environment to the susceptibility of austenitic stainless steels to corrosion. The relative humidity in the test environment is controlled by the water loading and the concentration of the hydrating salts such as $CaCl_2$. For each salt or salt mixture there is a threshold relative humidity below which the necessary liquid electrolyte cannot exist, and therefore below which the SCC risk is very low. This threshold is a thermodynamic quantity known as the deliquescence relative humidity that is dependent on the identity of the salt but is independent of the quantity of salt. Below the deliquescence RH there should be low corrosion risk, and above it the corrosion risk increases rapidly as a liquid phase, which is initially saturated with salt, grows and becomes more widespread in the container. At extremely high relative humidity the risk of corrosion decreases again due to the formation of less corrosive, dilute salt solutions. Additionally, if the hydrating salt content is high, all the moisture in the container may be consumed by the formation of the hydrate and the risk of corrosion will decrease because deliquescence cannot occur. The test results demonstrate that the risk of corrosion is function of the moisture and salt contents and other exposure variables that control the tendency for deliquescence and the formation of a corrosion supporting electrolyte on the metal surface.

ACKNOWLEDGEMENTS

Funding for this work was provided by the Surveillance and Monitoring Program, US Department of Energy Office of Environmental Management. This work was conducted at Los Alamos National Laboratory operated by Los Alamos National Security, LLC under contract DE-AC52-06NA25396 and at the Savannah River National Laboratory operated by Savannah River Nuclear Solutions for US Department of Energy under contract DE-AC09-08SR22470.

REFERENCES

1. Sedriks, A. J., *Corrosion of Stainless Steels*, 2nd edition, Wiley, New York, 1996.

2. Dunn, K. A., G. T. Chandler, C. W. Gardner, M.R. Louthan, J.W. McClard, and L. A. Worl. 2010. Supporting Safe Storage of Plutonium-Bearing Materials Through Science, Engineering and Surveillance. *Journal of Nuclear Materials Management* Vol. 37, No. 2

3. Veirs, D. K., L. A. Worl, D. M. Harradine, M. A. Martinez, R. S. Lillard, D. S. Schwartz, C. V. Puglisi, D. D. Padilla, A. Carrillo, R. E. McInroy, and A. R. Montoya, "Gas Generation and Corrosion in Salt-Containing Impure Plutonium Oxide Materials: Initial Results for ARF-102-85-223," LA-UR-04-1788, Los Alamos National Laboratory, Los Alamos, NM.

4. Zapp, P. E. and R. R. Livingston, "Corrosion Tests of 304L and 316L Stainless Steels for the 3013 Container," WSRC-TR-2005-00191, Savannah River National Laboratory, Aiken, SC, September 2005.

5. Shoji, Saburo and Noriyuki Ohnaka, *Boshoku Gijutsu* 38 (2) (1989) 92.

6. Lillard R. S., D. G. Kolman, M. A. Hill, M. B. Prime, D. K. Veirs, L. A. Worl, and P. E. Zapp, *Corrosion* 65 (3) (2009) 175.

7. P. E. Zapp, J. M. Duffey, K. A. Dunn, R. R. Livingston, and D. Z. Nelson, "Localized Corrosion of Austenitic Stainless Steel Exposed to Mixtures of Plutonium Oxide and Chloride Salts," CORROSION/2009, paper no. 09409.

8. P. S. Lam, P. E. Zapp, J. M. Duffey, and K. A. Dunn, *Proceedings of PVP2009 2009 ASME Pressure Vessels and Piping Division Conference*, Prague, Czech Republic, paper 77432.

9. ABAQUS Implicit Version 6.6.3, Dassault Systèmes Simulia Corporation (formerly ABAQUS Inc.), Providence, Rhode Island, 2008.

10. Mickalonis, J.I., K.A. Dunn. 2010. Residual Stresses in 3013 Containers. *Journal of Nuclear Materials Management* Vol. 37, No. 2